# Diagnostic Method for Measuring Plasma-Induced Voltages on the PBX-M Stabilizing Shell

PPPL--2711

DE90 013563

H. W. Kugel, M. Okabayashi, and S. Schweitzer

Princeton Plasma Physics Laboratory, Princeton University
Princeton, NJ 08544, USA

## ABSTRACT

The *Princeton* Beta Experiment-Modified (PBX-M) has a close-fitting, conducting, passive plate, stabilizing shell which nearly surrounds highly indented, bean-shaped plasmas. The proximity of this electrically isolated shell to a large fraction of the plasma surface allows measurements similar to previous work on other tokamaks using floating probes and limiters. Measurements were performed to characterize the plasma-induced voltages on the PBX-M passive plate stabilizing shell during high-$\beta$ plasmas. Voltage differences were measured between the respective passive plate toroidal and poloidal gaps, the respective passive plates and the vessel, and an outer poloidal graphite limiter and its passive plate. The calibration and qualification testing procedures are discussed. The initial measurements found that the largest voltages were observed at plasma start-up and at the plasma current disruption and exhibited characteristics depending on operating conditions. The highest voltages observed have been at disruption and were less than 2 kV

shows a partial schematic diagram of the passive plate system which is composed of five pairs of electrically isolated plates positioned above and below the magnetic axis. The outer two pairs of plates (labeled 1 and 2 in Fig. 2(a) perform stabilization of the n=1 kink modes. These plates are connected together electrically at 11 locations as shown in Fig. 2(b). The three inner pairs of plates [labeled 3, 4, and 5 in Fig. 2(a)] perform stabilization of the n=0 vertical modes and are connected electrically as shown in Fig. 2(c). Each plate has a toroidal OH gap. The plates consist of 2.5 cm thick aluminium with an explosively bonded layer of 0.32 cm thick stainless steel facing the plasma. The individual plate elements are supported from the vacuum vessel wall and electrically isolated using mica and alumina insulators. Wires from each of the five passive plate elements are connected to the vacuum vessel through 500 Ω bleed resistors which are external to the vessel. At 10 toroidal locations, an array of 2 cm high, electrically isolated, poloidal graphite limiters surrounds the plasma. Typically, the plasmas at start-up are near-circular in shape and are positioned on the outer limiters. Later in the discharge, highly indented bean-shaped plasmas are achieved and positioned for minimal contact with the poloidal limiters.

## III. EXPERIMENTAL PROCEDURE

Initial measurement surveys were performed using two high voltage probes with peak voltage ratings of 40 kV and signal attenuations of $10^{-4}$ The outputs of each probe were connected to two amplifiers to permit variable attenuations of the detected signals over a range from 1 to $10^3$ for simultaneous surveys over wide voltage ranges. The resultant output signals were connected to 10 V differential digitizers with adjustable digitization rates (40 to 100 kHz). Some scans were performed with the probe outputs connected to 3.5 MHz, latching peak detectors whose outputs were then digitized. These probes were connected sequentially between components expected to experience the highest voltage differences. No peak voltages higher than 2 kV were observed during these surveys. Typically the voltage durations were of order 300-400 msec. These 40 kV probe surveys provided an initial characterization of the passive plate voltage regime and demonstrated the utility of expanding the measurement system to assure complete coverage of voltage distributions arising from different disruption modes.

Using the results of the initial measurement surveys, an expanded voltage measuring system was implemented. This expanded voltage measurement system used teflon covered, twisted pairs of wires from the five passive plate elements, their respective toroidal gaps, the inter-element gaps, and an outer poloidal limiter. These wire pairs were brought outside the vessel and connected to an array of sixteen, 100 kΩ, compensated voltage dividers which provided output signals reduced by $10^{-3}$ and an output impedance of 100 Ω for direct connection to the differential digitizers. The system was referenced to ground via a connection at the digitizers to building steel. Each voltage divider was fabricated using, non-inductive 10 kΩ resistors in series. Each resistor was in parallel with a 100 pf capacitor. The compensated voltage dividers were adjusted to give attenuation ratios of 1:1000 to within an accuracy of $\pm$ 0.1%. In addition to direct voltage measurements, for some experiments, two peak detectors with a frequency response of 3.5 MHz were connected between the voltage divider outputs and the digitizers to survey for fast voltages as described above.

A principal instrumental concern was the validity and correct interpretation of the voltage measurements derived from signals originating from both low and high impedance sources in the PBX-M tokamak environment and transported through regions of possibly high electromagnetic interference. During normal operations, this environment included the presence of large voltages and currents, a high power neutral beam injection heating system, an IBW plasma current profile modification system, edge plasma effects, rotating machinery, and other noise sources. During plasma current disruptions higher than normal contributions were expected from some of these noise sources. Hence, an extensive series of tests, calibrations, and consistency checks were pursued to qualify the results and to understand possible limitations of the measurement system.

The continuity and polarity convention of the cabling from the passive plates to the data acquisition system were confirmed by placing a battery across the respective passive plate gaps in the vessel and measuring the system output voltage at the input and output of the data acquisition system. The Common Mode Rejection Ratio of the system was measured to be 2000:1 at 100 Hz and 1000:1 at 10 kHz. The passive plate toroidal gaps were low impedance voltage sources and the passive plate poloidal gaps were high impedance voltage sources. In order to check for possible voltage source impedance effects, tests were performed in which each voltage source was measured simultaneously with voltage divider ratios differing by a factor of 10 (*i.e.*, with total attenuations of $10^{-2}$ and $10^{-3}$, respectively). In all cases, the spectra were identical except for the factor of 10 difference. Magnetic field-only tests in the absence of plasma were performed daily to monitor the PBX-M control and diagnostic systems. These tests provided a check on the high voltage monitoring system. It was found that there were no induced signals aside from the small voltages induced at the start and finish of a constant applied field and that the signals were comparable to those induced in the flux loops. Reversing the direction of the applied field reversed the direction of the observed effects. Similar tests were made with each of the 7 shaping field systems of PBX-M, and with various combinations of these fields. The system voltage offsets were measured automatically before the beginning of each plasma pulse and used to correct the spectra measured during the plasma pulse.

## IV. RESULTS

Figure 3 shows typical voltage waveforms over the 500 msec, 400 kA, plasma pulse for (a) passive plate No. 5, toroidal gap, (b) the passive plate No. 2-No. 3, poloidal gap and (c) an outer poloidal limiter relative to passive plate No. 1. Plasma-induced voltages were seen at start-up and disruption. During the plasma pulse, the voltage differences were near zero except during small interactions of the edge plasma with the passive plates. This effect was most pronounced for the poloidal interplate gaps [*e.g.*, Fig. 3(b)]. Figure 4 shows the first 50 ms of these waveforms at start-up. All of the passive plate toroidal gaps [*e.g.*, Fig. 4(a)] exhibited a small induced voltage as the OH current ramp-up started. The passive plate poloidal gaps [*e.g.*, Fig.4(b)] exhibited a voltage difference on the order of several hundred volts which may to be related in part to run away electron effects and plasma motion as was also seen on the outer poloidal limiter [*e.g.*, Fig.4(c)]. The voltages on the outer poloidal limiter at breakdown were similar to those measured on other tokamak limiters at breakdown (100-800 V) and have been related in part to runaway electrons, arcing, and plasma motion [5-8]. Figure 5 shows the behavior of the same waveforms at disruption. The gap voltages appeared after the plasma interacted with the edge. This can be seen in Fig.5(e), which shows a central soft X-ray detector signal exhibit a growing mode which began to collapse at 472.2 ms followed by a final collapse. Passive plate voltages appeared as the outer soft X-ray detector signals saturated [*e.g.*, Fig.5(f)] and the plasma started moving vertically as indicated by the segmented flux loop difference signal [Fig. 5(d)]. The toroidal and poloidal gap voltage polarities changed as the plasma disruption motion changed. The plasma current (Ip) began to rise and then decay after the appearance of the voltages. The highest voltages observed have been at disruption and were less than 2 kV.

## ACKNOWLEDGMENTS

We wish to acknowledge technical contributions from L. Gereg, D. Moser, J. Semler, E. Thorsland, and the PBX-M technical staff. This work was supported by the United States Department of Energy Contract No. DE-ACO2-76-CHO-3073.

## REFERENCES

[1.] M. Okabayashi, *et al.*, in **Plasma Physics and Controlled Nuclear Fusion Research**, Proc. 12th Int. Conf., Nice, 1988 (IAEA, Vienna) **1**, 97 (1989).

[2.] R. E. Bell, *et al.* , Phys. Fluids (*to be published*, June 1990).

[3.] K. Bol, *et al.*, Phys. Rev. Lett.57, 1891 (1986).

[4.] H. W. Kugel, *et al.* , in **Controlled Fusion and Plasma Physics**, Proc. 16th Europ. Conf., Venice, March 1989, part **I**, Vol. 1, 199 (1989).

[5.] D.H.J. Goodall, J. Nucl. Mater. **93 &94**, 154 (1980)

[6.] P. Mioduszewski, R. E. Clausing, and L. Heatherly, J. Nucl. Mater. **85&86**, 963 (1979).

[7.] H. Ohtsuka, N. Ogiwara, and M. Maeno, J. Nucl. Mater. **93 & 94**, 161 (1980).

[8.] G. M. McCracken, J. Nucl. Mater. **93 & 94**, 3 (1980) and references therein.

[9] H. W. Kugel,*et al.* , to be published.

## FIGURE CAPTIONS

Fig. 1 Partial schematic cross section view of PBX-M showing the passive plate system and total flux contours for a discharge with $\beta_t$=6.8% and an indentation of 28%.

Fig. 2 Partial schematic view of the PBX-M passive plate system.

Fig. 3 Typical passive plate voltage waveforms for a 400 kA discharge. Shown are waveforms for (a) passive plate No. 5 toroidal gap, (b) passive plate No.2-No.3, poloidal gap, (c) an outer poloidal limiter relative to passive plate No.1, and (d) the plasma current (Ip).

Fig. 4 Typical passive plate voltage waveforms at start-up for a 400 kA discharge. Shown are waveforms for (a) passive plate No. 5 toroidal gap, (b) passive plate No.2-No.3, poloidal gap, (c) an outer poloidal limiter relative to passive plate No.1, (d) the ohmic current, and (e) the plasma current (Ip).

Fig. 5 Typical passive plate voltage waveforms at disruption for a 400 kA discharge. Shown are waveforms for (a) passive plate No. 5 toroidal gap, (b) passive plate No.2-No.3, poloidal gap, (c) an outer poloidal limiter relative to passive plate No.1, (d) a segmented flux loop difference, (e) a central soft X-ray detector (SXR), (f) an outer soft X-ray detector, and (g) the plasma current (Ip).

89X3393

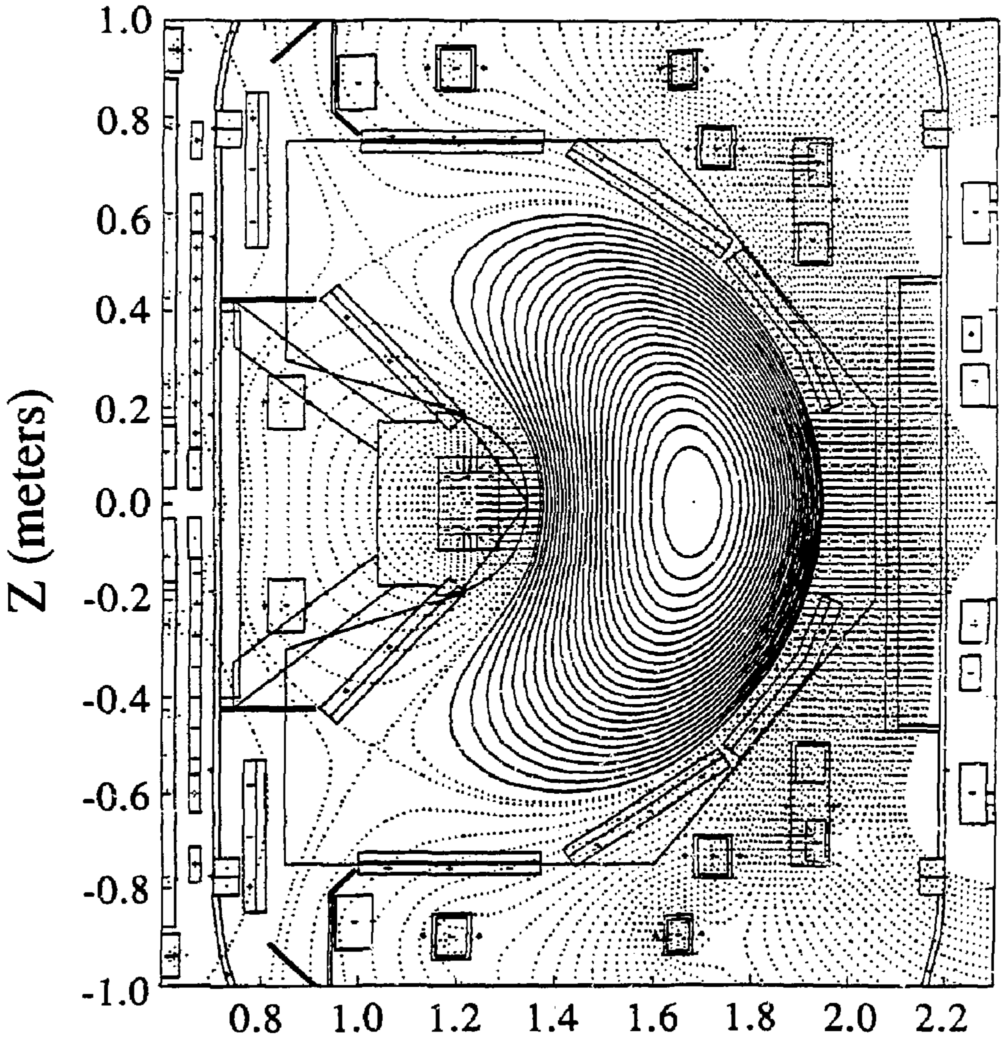


FIG. 1

#89X0549

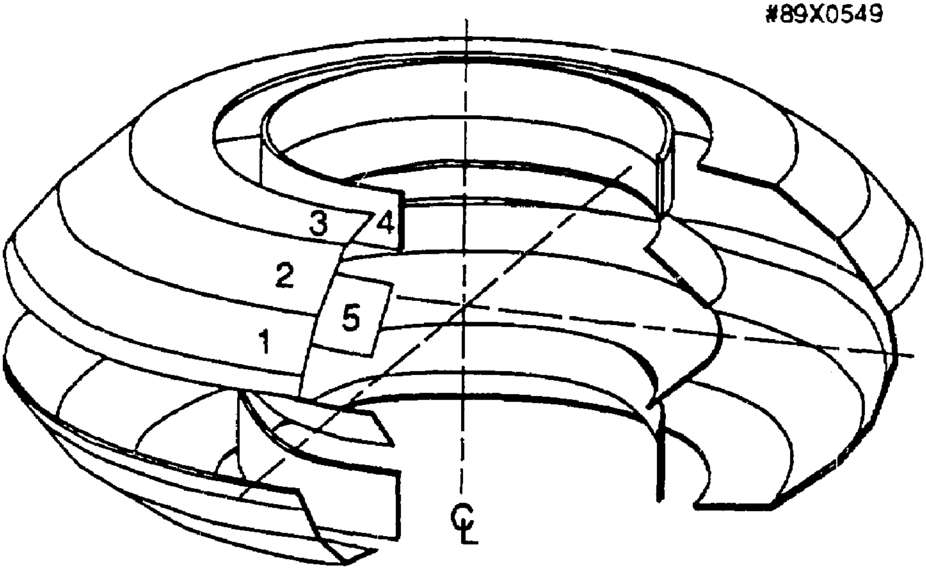


(a) Schematic view of PBX-M Passive Stabilizer

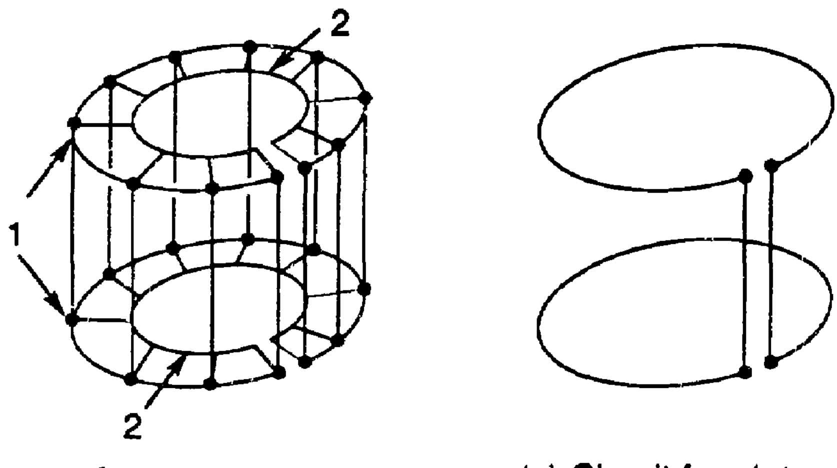


(b) Circuit for upper and lower plates No. 1 and 2

(c) Circuit for plates No. 3 - 5

FIG. 2

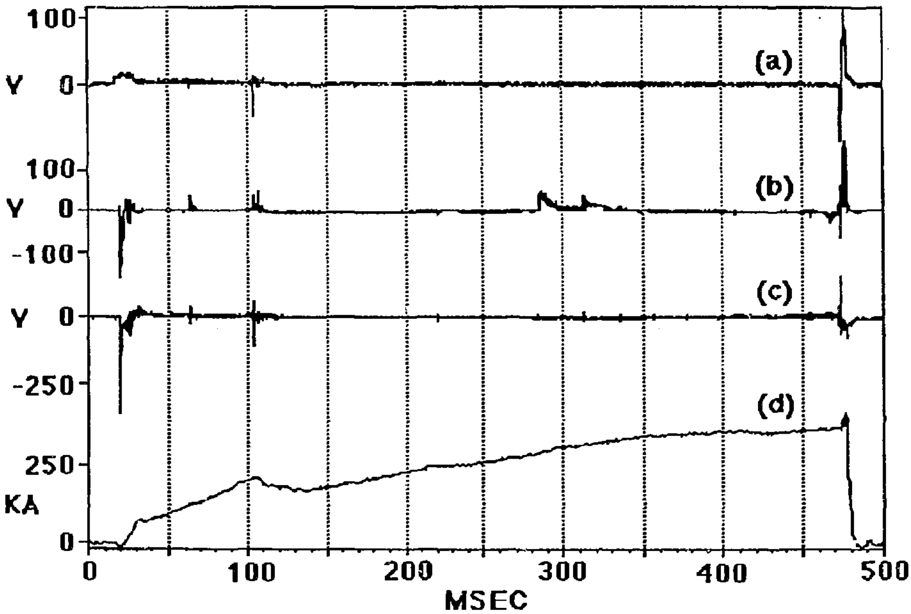


FIG. 3

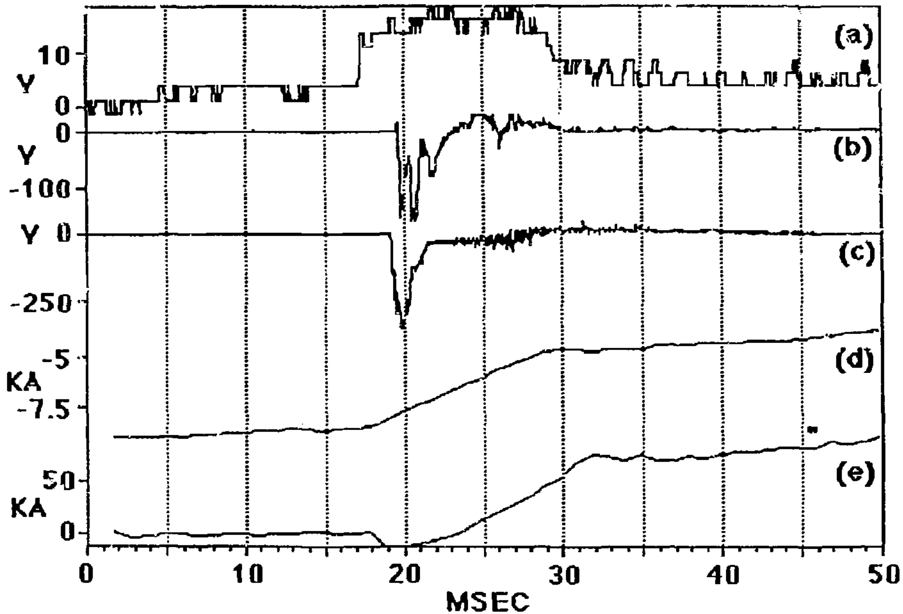


FIG. 4

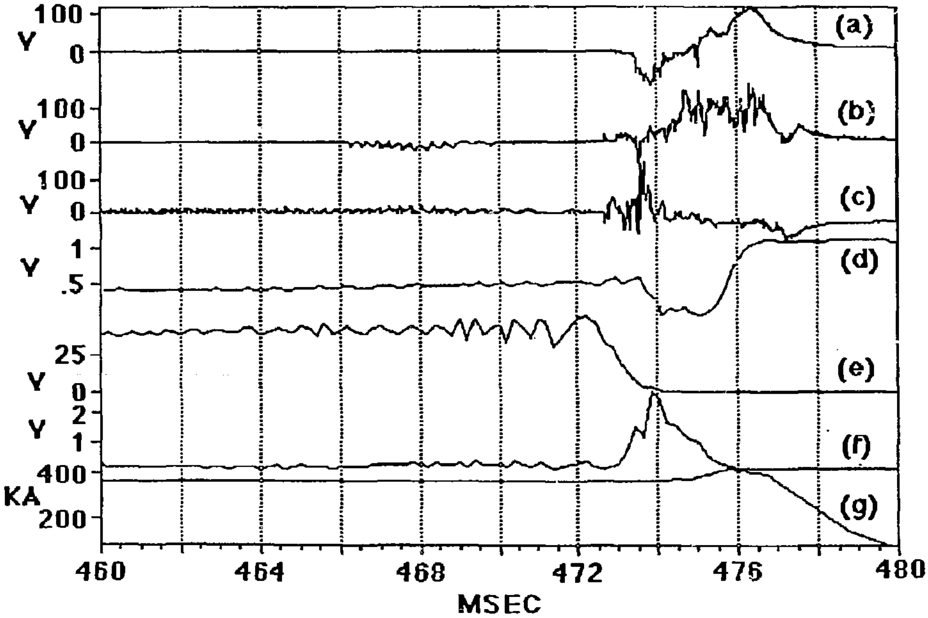

Y
100
0
(a)
Y
100
0
(b)
Y
100
0
(c)
Y
1
.5
(d)
25
Y
0
(e)
Y
2
1
(f)
400
KA
200
(g)
460
464
468
472
476
480
MSEC


FIG. 5

EXTERNAL DISTRIBUTION IN ADDITION TO UC-420

Dr. F. Paoloni, Univ. of Wollongong, AUSTRALIA
Prof. M.H. Brennan, Univ. of Sydney, AUSTRALIA
Plasma Research Lab., Australian Nat. Univ., AUSTRALIA
Prof. I.R. Jones, Flinders Univ, AUSTRALIA
Prof. F Cap, Inst. for Theoretical Physics, AUSTRIA
Prof. M. Heindler, Institut für Theoretische Physik, AUSTRIA
Prof. M. Goossens, Astronomisch Instituut, BELGIUM
Ecole Royale Militaire, Lab. de Phy. Plasmas, BELGIUM
Commission-European, DG. XII-Fusion Prog., BELGIUM
Prof. R. Boucique, Rijksuniversiteit Gent, BELGIUM
Dr. P.H. Sakanaka, Instituto Fisica, BRAZIL
Instituto De Pesquisas Espaciais-INPE, BRAZIL
Documents Office, Atomic Energy of Canada Ltd., CANADA
Dr. M.P. Bachynski, MPB Technologies, Inc., CANADA
Dr. H.M. Skarsgard, Univ. of Saskatchewan, CANADA
Prof. J. Teichmann, Univ. of Montreal, CANADA
Prof. S.R. Sreenivasan, Univ. of Calgary, CANADA
Prof. T.W. Johnston, INRS-Energie, CANADA
Dr. R. Bolton, Centre canadien de fusion magnétique, CANADA
Dr. C.R. James,, Univ. of Alberta, CANADA
Dr. P. Lukac, Komenskeho Universzita, CZECHOSLOVAKIA
The Librarian, Culham Laboratory, ENGLAND
Library, R61, Rutherford Appleton Laboratory, ENGLAND
Mrs. S.A. Hutchinson, JET Library, ENGLAND
P. Mähönen, Univ. of Helsinki, FINLAND
C. Mouttet, Lab. de Physique des Milieux Ionisés, FRANCE
J. Radet, CEN/CADARACHE - Bat 506, FRANCE
Ms. C. Rinni, Univ. of Ioannina, GREECE
Dr. T. Mual, Academy Bibliographic Ser., HONG KONG
Preprint Library, Hungarian Academy of Sci., HUNGARY
Dr. B. Das Gupta, Saha Inst. of Nuclear Physics, INDIA
Dr. P. Kaw, Inst. for Plasma Research, INDIA
Dr. P. Rosenau, Israel Inst. of Technology, ISRAEL
Librarian, International Center for Theo Physics, ITALY
Miss C. De Palo, Associazione EURATOM-ENEA , ITALY
Dr. G. Grosso, Istituto di Fisica del Plasma, ITALY
Dr. H. Yamato, Toshiba Res & Devel Center, JAPAN
Prof. I. Kawakami, Atomic Energy Res.Inst., JAPAN
Prof. K. Nishikawa, Hiroshima Univ., JAPAN
Director, Japan Atomic Energy Research Inst., JAPAN
Prof. S. Itoh, Kyushu Univ., JAPAN
Data and Planning Center, Nagoya Univ., JAPAN
Prof. S. Tanaka, Kyoto Univ., JAPAN
Library, Kyoto Univ., JAPAN
Prof. N. Inoue, Univ. of Tokyo, JAPAN
S. Mori, Technical Advisor, JAERI, JAPAN
O. Mitarai, Kumamoto Inst. of Technology, JAPAN
H. Jeong, Korea Advanced Energy Research Inst., KOREA
Prof. D.I. Choi, The Korea Adv. Inst. of Sci. & Tech., KOREA
Prof. B.S. Liley, Univ. of Waikato, NEW ZEALAND
Inst. of Plasma Physics, PEOPLE'S REPUBLIC OF CHINA
Librarian, Inst. of Physics, PEOPLE'S REPUBLIC OF CHINA
Library, Tsinghua Univ., PEOPLE'S REPUBLIC OF CHINA
Z. Li, S.W. Inst Physics, PEOPLE'S REPUBLIC OF CHINA
Prof. J.A.C. Cabral, Instituto Superior Tecnico, PORTUGAL
Dr. O. Petrus, AL I CUZA Univ., ROMANIA
Dr. J. de Villiers, Fusion Studies, AEC, S. AFRICA
Prof. M.A. Hellberg, Univ. of Natal, S. AFRICA
C.I.E.M.A.T, Fusion Division Library, SPAIN
Dr. L. Stenflo, Univ. of UMEA, SWEDEN
Library, Royal Inst. of Technology, SWEDEN
Prof. H. Wilhelmson, Chalmers Univ. of Tech., SWEDEN
Centre Phys. Des Plasmas, Ecole Polytech, SWITZERLAND
Bibliotheek, Inst. Voor Plasma-Fysica, THE NETHERLANDS
M. Durgut, Vice Chairman, Middle East Tech. Univ., TURKEY
Dr. D.D. Ryutov, Siberian Branch of Academy of Sci., USSR
Dr. G.A. Eliseev, Kurchatov Inst., USSR
Librarian, The Ukr.SSR Academy of Sciences, USSR
Dr. L.M. Kovrizhnykh, Inst. of General Physics, USSR
Kernforschungsanlage GmbH, Zentralbibliothek, W. GERMANY
Bibliothek, Inst. Für Plasmaforschung, W. GERMANY
Prof. K. Schindler, Ruhr-Universität Bochum, W. GERMANY
Dr. F. Wagner, (ASDEX), Max-Planck-Institut, W. GERMANY
Librarian, Max-Planck-Institut, W. GERMANY
Prof. R.K. Janev, Inst. of Physics, YUGOSLAVIA